

Research Article

Optimal Scheduling Strategy for Regional Microgrid considering Large-Scale Access of Electric Vehicles

Tengfei Zhang ¹, Yiling Cheng ¹, Chen Peng,² Fumin Ma,³ Deliang Zeng,⁴ and Gregory M. P. O'Hare⁵

¹College of Automation & Artificial Intelligence, Nanjing University of Posts and Telecommunications, Nanjing 210023, China

²School of Mechatronic Engineering and Automation, Shanghai University, Shanghai 200072, China

³College of Information Engineering, Nanjing University of Finance and Economics, Nanjing 210023, China

⁴State Key Laboratory of Alternate Electrical Power System with Renewable Energy Sources, North China Electric Power University, Beijing 102206, China

⁵School of Computer Science and Statistics, Trinity College Dublin, Dublin 2, Ireland

Correspondence should be addressed to Tengfei Zhang; tfzhang@126.com

Received 8 June 2022; Revised 4 August 2022; Accepted 23 August 2022; Published 22 September 2022

Academic Editor: N. Prabaharan

Copyright © 2022 Tengfei Zhang et al. This is an open access article distributed under the Creative Commons Attribution License, which permits unrestricted use, distribution, and reproduction in any medium, provided the original work is properly cited.

In recent years, renewable energy, especially photovoltaic (PV) generation, has been widely applied in commercial and residential areas, forming the structure of regional microgrids (MG). On the other hand, as large-scale electric vehicles (EVs) are connected to the regional MG, their disordered charging and discharging will enable extremely bad effects. However, most of the existing scheduling strategies focused on a single MG or considered the MG as a single node, ignoring the characteristics of different subareas. To address these limitations, we propose an optimal scheduling strategy considering large-scale access of EVs based on the typical regional MG composed of commercial and residential subareas, combining the power consumption characteristics of the two subareas and the travel characteristics of EVs. This strategy is mainly to dynamically adjust the charging and discharging of EVs in each subarea, combined with the real-time deployment of excess PV energy, so as to realize the overall scheduling of the regional MG. Numerical results show that EVs store electric energy during valley hours and output electric energy during peak hours. Furthermore, compared with no scheduling method, the proposed strategy reduces the whole-day electricity bills of the regional MG.

1. Introduction

The extensive use of fossil fuels has caused serious environmental problems and energy crises [1]. In order to reduce the dependence on fossil fuels and build up a low-carbon energy system, the development and utilization of clean, renewable energy sources (RESs), such as solar energy, has growingly big appeals [2, 3]. By collecting, storing, and using RESs locally, microgrids (MGs) can effectively deal with the randomness and intermittence of RESs [4, 5], which has become the most important means to alleviate the problem with RESs consumption and interact with power grids friendly. On the other hand, with the growth of the electric vehicle (EV) industry, the large-scale access of EVs will bring

great negative impacts on the operation of power grids. The State Council and the Ministry of Industry and Information Technology of China foresee that the sales of new energy EVs in China will reach 20% of the total vehicle sales by 2025 [6]. In Reference [7], it is pointed out that EVs without regulation will lead to an increase in electricity demands, electricity prices, and greenhouse gas emissions. However, it is worth noting that civilian vehicles are parking more than 90% of the time each day [8]. They have the potential to participate in MG power regulation as distributed mobile energy storage.

The basic idea of Vehicle-to-Grid (V2G) technology is to integrate battery vehicles (BVs) into power grids to serve as controllable loads or energy supply/storage facilities [9, 10].

In Refs. [11, 12], the scheme of EVs providing spinning reserves is discussed. In Refs. [13–15], the authors present the strategy for EVs to participate in frequency modulation. References [16–18] propose the congestion management mechanism by using EVs. In Ref. [19], the impact of EVs' charging-discharging behavior on the economic benefits of MG is analyzed.

In MG operation, EVs are always involved in power regulation, mainly by such means as peak shaving, valley filling, and excess renewable energy consumption. In this regard, the authors in Ref. [20] propose two decentralized EV charge scheduling schemes for shaping the load curve of residential communities, which coordinate valley filling and peak shaving via both EV charging and discharging. In Ref. [21], the authors propose an integrated management schedule for EVs to address the issues such as battery charging, electric price, and availability of electric stations. Based on a community integrated energy system, Ref. [22] presents an optimal dispatching model for EVs to coordinate flexible demand response and multiple renewable uncertainties. The authors in Ref. [23] propose a real-time EV charging management scheme for commercial buildings with photovoltaic (PV) generation and EV charging services, which can handle the uncertainties of PV generation and EV parking optimally. In Ref. [24], it is proved that solar V2G parking lots can reduce the power consumption pressure during peak hours and provide electric energy when necessary. However, the focus of Ref. [24] is on the instantaneous state, and no complete charge-discharge control strategy is discussed.

When EVs participate in regulation, the electricity consumption characteristics of residents also need to be considered. Reference [25] designs a regulation strategy for adding PV generations and V2G. It points out that in summer, PV generations can sometimes fully meet the electricity demands of residents during the daytime. It also points out that there is a potential for EVs to stabilize the grid in regard of peak-load shaving. Specifically, the authors in Ref. [26] propose a demand response algorithm to control the charging and discharging of EVs within different districts.

In actual applications, some adjacent areas, such as residential and commercial areas, may compose a regional MG. These different subareas usually have complementary power consumption characteristics, and the travel behavior of EVs will lead to certain coupling relationships between different subareas, or even different regional microgrids. The above studies have deeply analyzed the potential of EVs in MG regulation. However, all of them are focused on a single MG, lack consideration of multiple related regional MGs, and rarely explore the coordination between different subareas within a regional MG. In order to solve the above problems, this paper studies the ubiquitous regional MG composed of residential and commercial subareas and proposes an optimal scheduling strategy by regarding large-scale EVs as mobile energy storage. In the proposed strategy, we consider the issues such as the power consumption characteristics of different subareas, the travel characteristics of EVs, and the uncertainties of PV generation. The system

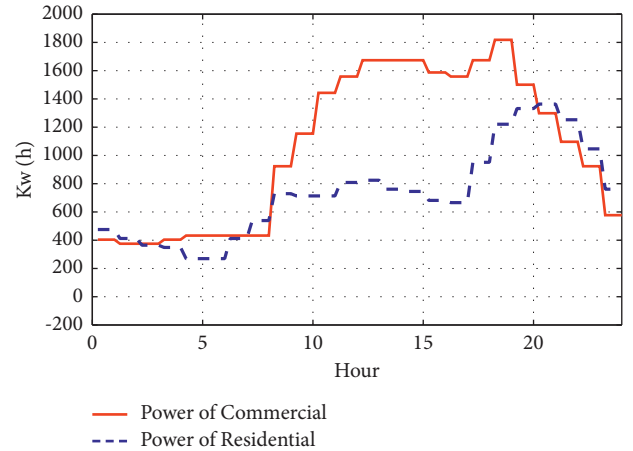


FIGURE 1: Commercial and residential load demands.

can realize the complementary optimal scheduling between different subareas.

The main contributions of this paper are listed as follows:

- (1) For the regional MG composed of commercial and residential subareas, an optimal scheduling architecture is developed, under which EVs are regarded as mobile energy storages. Further, an optimal scheduling strategy is proposed.
- (2) The power consumption characteristics of two subareas and the travel characteristics of EVs are analyzed. EVs store cheap electric energy during valley hours and discharge the subarea in need for a short time during peak hours. Combined with the real-time deployment of PV energy, the complementary scheduling of the regional MG is realized.
- (3) The power consumption models of two subareas and the charge-discharge model of EVs are established. Dynamically adjusting the charging-discharging of EVs in each subarea according to the PV situation and specific electricity demand so as to realize peak shaving, valley filling, and economic operation of the regional MG. The discharging of EVs can also reduce power fluctuations.

The rest of this paper is organized as follows: Section 2 develops the optimal scheduling architecture. In Section 3, the power consumption models of commercial and residential areas and the charge-discharge model of EVs are established. Section 4 proposes the optimal scheduling strategy. The simulations are performed in Section 5, and the conclusion is reached in Section 6.

2. Regional MG Optimal Scheduling Architecture

Urban residents' production, life, entertainment, and other activities are geographically and temporally concentrated, creating different types of areas, such as industrial, residential, and commercial areas. In addition, there is also a case that residential areas and nearby commercial areas form

a regional MG because residential areas and commercial areas have certain complementary characteristics in terms of electricity consumption and EV parking, which bring a possibility for formulating the corresponding optimal scheduling strategy.

Typical commercial and residential load demands are shown in Figure 1 [27]. Generally, due to the work needs of residents, the commercial load demand is significantly higher during 10:00–19:00, and the peak periods are 11:00–19:00. At night, residents return to residential areas, so the residential load demand rises rapidly; as can be seen, the peak periods are 18:00–23:00. From midnight to early morning (00:00–08:00), the commercial and residential load demands are both low.

On the other hand, during the daytime, there are many EVs parking in commercial areas. In order to avoid the case that the charging demands of EVs further drive up the power consumption pressure, the charging of EVs should be managed and the traditional free charging mode should be improved. At night, EVs will return to residential areas, and the charging demands of EVs will also deliver great pressure without management.

Based on the MG pattern of “commercial areas + residential areas,” this paper proposes a regional MG scheduling strategy considering large-scale access of EVs. The scheduling can be optimized by using different control strategies for different subareas and referring to the mobile energy storage characteristics of EVs.

When both commercial and residential areas are allocated with PV generations, residential areas with low electricity demand can provide excess PV energy to commercial areas when a surplus of PV power is available. And during the peak hours in commercial areas, EVs with a higher state of charge (SOC) in commercial areas can be allowed to transmit part of their electric energy into the regional MG so as to realize peak shaving.

At night, PV generations can no longer work. On the other hand, residential areas are in night peak hours. Because private vehicles almost have no travel needs at night, EVs with higher SOC in residential areas are allowed to transmit part of their electric energy into the regional MG, thus realizing peak shaving and reducing electricity bills. From midnight to early morning, the regional MG electricity demand drops to a low level, while the electricity prices are low. Through regulation, the charging demands of EVs in residential areas would be met as much as possible, and the energy storage characteristics of EVs can be fully exploited to deliver the effect of valley filling while being prepared for the discharging task during peak hours of the next day, finally creating a virtuous cycle.

Based on the above analyses, the regional MG optimal scheduling architecture considering large-scale access of EVs is shown in Figure 2.

3. Mathematical Model

To facilitate modeling and analysis, α and β are used to represent commercial and residential areas in a regional MG, respectively.

3.1. Power Consumption Model of Commercial Areas. Defining $P_C^{(\alpha)}$ and $P_O^{(\alpha)}$ as the power consumed and obtained by commercial areas, respectively, according to the power balance:

$$P_C^{(\alpha)} = P_O^{(\alpha)}, \quad (1)$$

where $P_C^{(\alpha)}$ includes the power consumed by commercial buildings $P_{\text{Building}}^{(\alpha)}$ and the charging power of commercial parking lots $P_{\text{C-Lot}}^{(\alpha)}$, that is,

$$P_C^{(\alpha)} = P_{\text{Building}}^{(\alpha)} + P_{\text{C-Lot}}^{(\alpha)}. \quad (2)$$

Because residential areas can transmit excess PV power to commercial areas, so $P_O^{(\alpha)}$ can be expressed as follows:

$$P_O^{(\alpha)} = P_{\text{PV}}^{(\alpha)} + P_{\text{PVex}}^{(\beta)} + P_{\text{D-Lot}}^{(\alpha)} + P_{\text{Grid}}^{(\alpha)}, \quad (3)$$

where $P_{\text{PV}}^{(\alpha)}$ is the PV power in commercial areas; $P_{\text{PVex}}^{(\beta)}$ is the excess PV power imported from residential areas, $P_{\text{PVex}}^{(\beta)} \geq 0$; $P_{\text{D-Lot}}^{(\alpha)}$ is the discharging power of commercial parking lots; $P_{\text{Grid}}^{(\alpha)}$ is the power imported from power grid. Replacing (2) and (3) into (1) can get the following:

$$P_{\text{Building}}^{(\alpha)} + P_{\text{C-Lot}}^{(\alpha)} = P_{\text{PV}}^{(\alpha)} + P_{\text{PVex}}^{(\beta)} + P_{\text{D-Lot}}^{(\alpha)} + P_{\text{Grid}}^{(\alpha)}. \quad (4)$$

3.2. Power Consumption Model of Residential Areas. Similarly, the power consumption model of residential areas can be obtained:

$$P_C^{(\beta)} = P_O^{(\beta)}, \quad (5)$$

where $P_C^{(\beta)}$ and $P_O^{(\beta)}$ are the power consumed and obtained by residential areas respectively, which can be expressed as follows:

$$P_C^{(\beta)} = P_{\text{Building}}^{(\beta)} + P_{\text{C-Lot}}^{(\beta)}, \quad (6)$$

$$P_O^{(\beta)} = P_{\text{PV}}^{(\beta)} + P_{\text{D-Lot}}^{(\beta)} + P_{\text{Grid}}^{(\beta)} - P_{\text{PVex}}^{(\beta)}, \quad (7)$$

where $P_{\text{Building}}^{(\beta)}$ is the power consumed by residential buildings; $P_{\text{C-Lot}}^{(\beta)}$ is the charging power of residential parking lots; $P_{\text{D-Lot}}^{(\beta)}$ is the discharging power of residential parking lots; $P_{\text{Grid}}^{(\beta)}$ is the power imported from power grid; $P_{\text{PV}}^{(\beta)}$ is the PV power in residential areas; $P_{\text{PVex}}^{(\beta)}$ is the excess PV power:

$$P_{\text{PVex}}^{(\beta)} = P_{\text{PV}}^{(\beta)} - P_C^{(\beta)}, \quad (8)$$

$$P_{\text{PVex}}^{(\beta)} \geq 0.$$

Note that $P_{\text{PVex}}^{(\beta)}$ means excess PV power, then $P_{\text{PVex}}^{(\beta)}$ and $P_{\text{Grid}}^{(\beta)}$ will not be greater than 0 at the same time. That is, it is not economical to transmit power to commercial areas while importing power from the power grid.

Replacing (6) and (7) into (5) can get the following:

$$P_{\text{Building}}^{(\beta)} + P_{\text{C-Lot}}^{(\beta)} = P_{\text{PV}}^{(\beta)} + P_{\text{D-Lot}}^{(\beta)} + P_{\text{Grid}}^{(\beta)} - P_{\text{PVex}}^{(\beta)}. \quad (9)$$

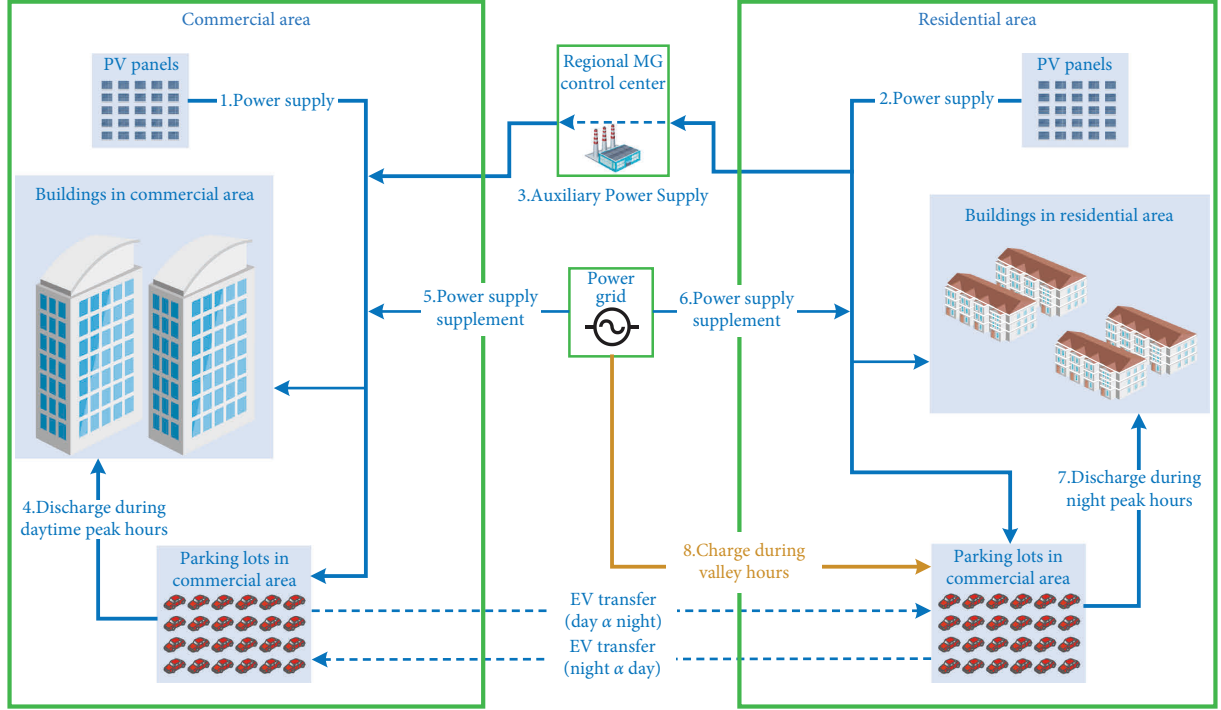


FIGURE 2: Regional MG optimal scheduling architecture.

3.3. Charge-Discharge Model of EVs

3.3.1. *Model of EVs in Commercial Areas.* During early morning and night, the PV generations can not work, and the EVs are concentrated in residential areas, so the regulation on commercial areas focused on the daytime peak hours.

The capacity of each vehicle is L , EVs in the commercial parking lots are divided into three categories according to their charging demands, and the classification is updated per 15 minutes. On this basis, a charging queue is sorted by SOC from low to high. Let SOC_L and $SOC_{H\alpha}$ represent two adjustable values, respectively. The classification details are as follows:

Lv1: EVs in urgent need of charging, i.e., $SOC \leq SOC_L$. EVs in Lv1 should all be charged and $P_{C_Lv1}^{(\alpha)}$ is the total charging power of the EVs in Lv1.

Lv2: EVs that are not in urgent need of charging, i.e., $SOC_L \leq SOC$. When there is a surplus of PV power in commercial areas: $P_{PV}^{(\alpha)} + P_{PVex}^{(\beta)} > P_{Building} + P_{C_Lv1}^{(\alpha)}$, EVs in Lv2 can be partly charged to consume the excess PV power, and $P_{C_Lv2}^{(\alpha)}$ is the total charging power of EVs in Lv2.

Lv3: EVs that can discharge, i.e., $SOC_{H\alpha} \leq SOC$. Short-time discharging can be performed during peak hours to reduce electricity bills in commercial areas. It is worth noting that Lv3 is a subcategory of Lv2.

Suppose there are $n_1^{(\alpha)}$ EVs in Lv1, $1 \leq i \leq n_1^{(\alpha)}$, the charging power of the i th EV is $P_{C_Lv1-j}^{(\alpha)}$; there are $n_2^{(\alpha)}$ EVs in Lv2, $1 \leq j \leq n_2^{(\alpha)}$, the charging power of the j th EV is $P_{C_Lv2-j}^{(\alpha)}$; there are $n_3^{(\alpha)}$ EVs in Lv3, $1 \leq k \leq n_3^{(\alpha)} \leq n_2^{(\alpha)}$, the SOC of the

k th EV is $SOC_{Lv3-k}^{(\alpha)}$, the discharging power is $P_{D_Lv3-k}^{(\alpha)}$. $P_{C_Lv1}^{(\alpha)}$ can be expressed as follows:

$$P_{C_Lv1}^{(\alpha)} = \sum_{i=1}^{n_1^{(\alpha)}} P_{C_Lv1-i}^{(\alpha)}. \quad (10)$$

According to the above classifications, we can express $P_{C_Lot}^{(\alpha)}$ as follows:

$$P_{C_Lot}^{(\alpha)} = P_{C_Lv1}^{(\alpha)} + P_{C_Lv2}^{(\alpha)} = \begin{cases} P_{C_Lv1}^{(\alpha)}, & \text{Limit}\alpha \leq P_{C_Lv1}^{(\alpha)}, \\ \text{Limit}\alpha, & P_{C_Lv1}^{(\alpha)} > \text{Limit}\alpha, \end{cases} \quad (11)$$

where $\text{Limit}\alpha = P_{PV}^{(\alpha)} + P_{PVex}^{(\beta)} - P_{Building}$. So $P_{C_Lv2}^{(\alpha)}$ can be expressed as follows:

$$P_{C_Lv2}^{(\alpha)} = \text{Limit}\alpha - P_{C_Lv1}^{(\alpha)} \leq \sum_{j=1}^{n_2^{(\alpha)}} P_{C_Lv2-j}^{(\alpha)}. \quad (12)$$

In order to evenly distribute discharging power during peak hours and refer to the calculation form of EV charging-discharging power in Ref. [28], we have the following:

$$P_{D_Lot}^{(\alpha)}(t) = \begin{cases} \frac{\sum_{k=1}^{n_3^{(\alpha)}} (SOC_{Lv3-k}^{(\alpha)} - SOC_{H\alpha}) \cdot L}{t_{p\ d-\alpha} - t}, & t \in \text{peak hours}, \\ 0, & t \notin \text{peak hours}, \end{cases} \quad (13)$$

$$P_{D_Lot}^{(\alpha)} \leq \sum_{k=1}^{n_3^{(\alpha)}} P_{D_Lv3_k}^{(\alpha)}, \quad (14)$$

where $t_{pd_α}$ is the end of the peak hours in commercial areas.

Meanwhile, in order to avoid grid fluctuations caused by a large number of EVs being discharged at the same time, it should be ensured that

$$P_{D_Lot}^{(\alpha)} (t) \leq P_{Building}^{(\alpha)} (t) + P_{C_Lv1}^{(\alpha)} (t) - \left[P_{PV}^{(\alpha)} (t) + P_{PVex}^{(\beta)} (t) + P_{Grid}^{(\alpha)} (t-1) \right]. \quad (15)$$

That is, in commercial areas, after EVs are discharged at t , the power $P_{Grid}^{(\alpha)} (t)$ imported from power grid at t is not higher than the power $P_{Grid}^{(\alpha)} (t-1)$ imported from power grid at the previous time $(t-1)$.

3.3.2. Model of EVs in Residential Areas. Similarly, EVs in the residential parking lots are also divided into the above

$$P_{C_Lot}^{(\beta)} = P_{C_Lv1}^{(\beta)} + P_{C_Lv2}^{(\beta)} = \begin{cases} P_{C_Lv1}^{(\beta)}, & \text{Limit}\beta \leq P_{C_Lv1}^{(\beta)}, \\ \text{Limit}\beta, & P_{C_Lv1}^{(\beta)} < \text{Limit}\beta \leq \sum_{i=1}^{n_1^{(\beta)}} P_{C_Lv1_i}^{(\beta)} + \sum_{j=1}^{n_2^{(\beta)}} P_{C_Lv2_j}^{(\beta)}, \\ & \sum_{i=1}^{n_1^{(\beta)}} P_{C_Lv1_i}^{(\beta)} + \sum_{j=1}^{n_2^{(\beta)}} P_{C_Lv2_j}^{(\beta)} < \text{Limit}\beta, \end{cases} \quad (17)$$

where $\text{Limit}\beta = P_{PV}^{(\beta)} - P_{Building}^{(\beta)}$, $P_{C_Lv1}^{(\alpha)}$ and $P_{C_Lv2}^{(\alpha)}$ are the total charging power of EVs in Lv1 and Lv2, respectively, which can be expressed as follows:

$$P_{C_Lv1}^{(\beta)} = \sum_{i=1}^{n_1^{(\beta)}} P_{C_Lv1_i}^{(\beta)}, P_{C_Lv2}^{(\beta)} = \text{Limit}\beta - P_{C_Lv1}^{(\beta)} \leq \sum_{j=1}^{n_2^{(\beta)}} P_{C_Lv2_j}^{(\beta)}. \quad (18)$$

When $\sum_{i=1}^{n_1^{(\beta)}} P_{C_Lv1_i}^{(\beta)} + \sum_{j=1}^{n_2^{(\beta)}} P_{C_Lv2_j}^{(\beta)} < \text{Limit}\beta$, it shows that there is a surplus of PV power in residential areas, the excess PV power $P_{PVex}^{(\beta)}$ can be calculated as follows:

$$P_{PVex}^{(\beta)} = \text{Limit}\beta - \sum_{i=1}^{n_1^{(\beta)}} P_{C_Lv1_i}^{(\beta)} + \sum_{j=1}^{n_2^{(\beta)}} P_{C_Lv2_j}^{(\beta)}. \quad (19)$$

In order to evenly distribute charging power, we have the following:

three categories according to their charging demands, and $\text{SOC}_{H\beta}$ is the boundary between Lv2 and Lv3.

Suppose there are $n_1^{(\beta)}$ EVs in Lv1, $1 \leq i \leq n_1^{(\beta)}$, the charging power of the i th EV is $P_{C_Lv1_i}^{(\beta)}$; there are $n_2^{(\beta)}$ EVs in Lv2, $1 \leq j \leq n_2^{(\beta)}$, the charging power of the j th EV is $P_{C_Lv2_j}^{(\beta)}$; there are $n_3^{(\beta)}$ EVs in Lv3, $1 \leq k \leq n_3^{(\beta)} \leq n_2^{(\beta)}$, the SOC of the k th EV is $\text{SOC}_{Lv3_k}^{(\beta)}$, the discharging power is $P_{D_Lv3_k}^{(\beta)}$.

During the early morning (valley hours), the electricity prices are low and there is no PV power. It is suitable to use the power grid to charge all EVs, so

$$P_{C_Lot}^{(\beta)} = \sum_{i=1}^{n_1^{(\beta)}} P_{C_Lv1_i}^{(\beta)} + \sum_{j=1}^{n_2^{(\beta)}} P_{C_Lv2_i}^{(\beta)}. \quad (16)$$

During daytime peak hours, $P_{C_Lot}^{(\beta)}$ can be expressed as follows:

$$P_{C_Lv2}^{(\beta)} = \begin{cases} \text{Limit}\beta - P_{PVex}^{(\beta)} - P_{C_Lv1}^{(\beta)}, & t \notin \text{valleyhours}, \\ \frac{\sum_{j=1}^{n_2^{(\beta)}} (\text{SOC}_{\text{stop}} - \text{SOC}_{Lv2_j}^{(\beta)}) \cdot L}{t_{vd_β} - t}, & t \in \text{valleyhours}, \end{cases} \quad (20)$$

where $t_{vd_β}$ is the end of the valley hours in residential areas; $\text{SOC}_{Lv2_j}^{(\beta)}$ is the SOC of the j th EV in Lv2; SOC_{stop} is the expected SOC of each EV at $t_{vd_β}$.

During night peak hours, PV generations stop working, and EVs in residential areas can realize peak shaving by discharging. For $P_{D_Lot}^{(\beta)}$, in order to evenly distribute discharging power during night peak hours, we have the following:

$$P_{D_Lot}^{(\beta)} (t) = \begin{cases} \frac{\sum_{k=1}^{n_3^{(\beta)}} (\text{SOC}_{Lv3_k}^{(\beta)} - \text{SOC}_{H\beta}) \cdot L}{t_{pd_β} - t}, & t \in \text{peakhours}, \\ 0, & \text{else,} \end{cases} \quad (21)$$

$$P_{D_Lot}^{(\beta)} \leq \sum_{k=1}^{n_3^{(\beta)}} P_{D_Lv3,k}^{(\beta)}, \quad (22)$$

where $t_{pd_β}$ is the end of the peak hours in residential areas.

Meanwhile, in order to avoid grid fluctuations caused by a large number of EVs being discharged at the same time, it should be ensured that

$$P_{D_Lot}^{(\beta)}(t) \leq P_{Building}^{(\beta)}(t) + P_{C_Lv1}^{(\beta)}(t) - [P_{PV}^{(\beta)}(t) + P_{Grid}^{(\beta)}(t-1)]. \quad (23)$$

That is, in residential areas, after EVs are discharged at t , the power $P_{Grid}^{(\beta)}(t)$ imported from power grid at t is not higher than the power $P_{Grid}^{(\beta)}(t-1)$ imported from the power grid at the previous time $(t-1)$.

4. Regional MG Optimal Scheduling Strategy

Assuming that both commercial and residential areas are equipped with PV panels, the PV power is preferentially used; and EVs in commercial and residential areas are parked centrally and can accept charging-discharging regulations. According to the load characteristics of the regional MG, the following optimal scheduling strategy is formulated:

- (1) Any subarea should ensure the load of buildings and the charging demands of EVs in Lv1, i.e.,

$$\begin{cases} P_C^{(\alpha)} \leq P_{Building}^{(\alpha)} + P_{C_Lv1}^{(\alpha)}, \\ P_C^{(\beta)} \leq P_{Building}^{(\beta)} + P_{C_Lv1}^{(\beta)}, \end{cases} \quad (24)$$

- (2) For any subarea, when the PV power is still surplus on the basis of (1), charging as many EVs in Lv2 as possible. The charging queue is sorted by SOC from low to high and updated per 15 minutes.
- (3) When the PV power in residential areas has a surplus on the basis of (2), that is, when $\sum_{i=1}^{n_1^{(\beta)}} P_{C_Lv1,i}^{(\beta)} + \sum_{j=1}^{n_2^{(\beta)}} P_{C_Lv2,j}^{(\beta)} < \text{Limit}\beta$, it is allowed to transmit the excess PV power $P_{PVex}^{(\beta)}$ to commercial areas according to equation (8).
- (4) For any subarea, when it is not in peak hours and the available PV power cannot meet the electricity demand, it should import power from the power grid. For commercial areas, if $P_{PV}^{(\alpha)} + P_{PVex}^{(\beta)} < P_{Building}^{(\alpha)} + P_{C_Lv1}^{(\alpha)}$, importing power from the power grid. For residential areas, if $P_{PV}^{(\beta)} < P_{Building}^{(\beta)} + P_{C_Lv1}^{(\beta)}$, importing power from the power grid.
- (5) For commercial areas, only during peak hours, when the available PV power can not meet the electricity demand, EVs still in the area with high SOC are allowed to discharge according to equations (13)–(15), and the power imported from the power grid is calculated according to equation (4). For

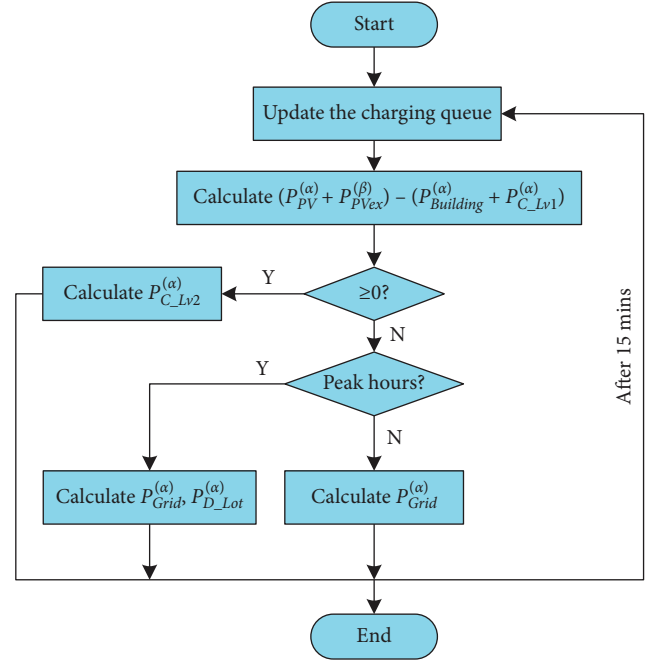


FIGURE 3: Calculation flowchart of commercial areas.

residential areas, only during night peak hours, EVs still in the area with high SOC are allowed to discharge for a short time according to equations (21)–(23), and the power imported from the power grid is calculated according to equation (9). The discharging electricity price is set to be the same as the flat hours.

- (6) In valley hours, making full use of cheap electric energy to charge EVs in residential areas, according to (16). If possible, make the SOC of each EV reach the expected value before the next day.

According to the above optimal scheduling strategy, the calculation flowcharts per 15 minutes of commercial and residential areas are shown in Figures 3 and 4.

5. Model Simulation

5.1. EV Behavior Analysis. In a regional MG, the distance between residential areas and commercial areas is short, generally only 1–3 km. From the perspective of work, only a small part of EVs leaving residential areas during the daytime will go to nearby commercial areas, and most of the rest will go to other commercial areas 10 km or even 20 km away. Similarly, only a small part of EVs returning to residential areas at night come from nearby commercial areas. In order to explore the effect of the proposed scheduling strategy, it is assumed that the strategy is not only implemented in a single regional MG but is widely used in an MG cluster.

As shown in Figure 5, the controlled area is simplified into three regional MGs with the same power consumption characteristics but at a distance from each other, namely three regional MGs: MG A, B, and C. Then, if there are several commercial areas or residential areas in a regional

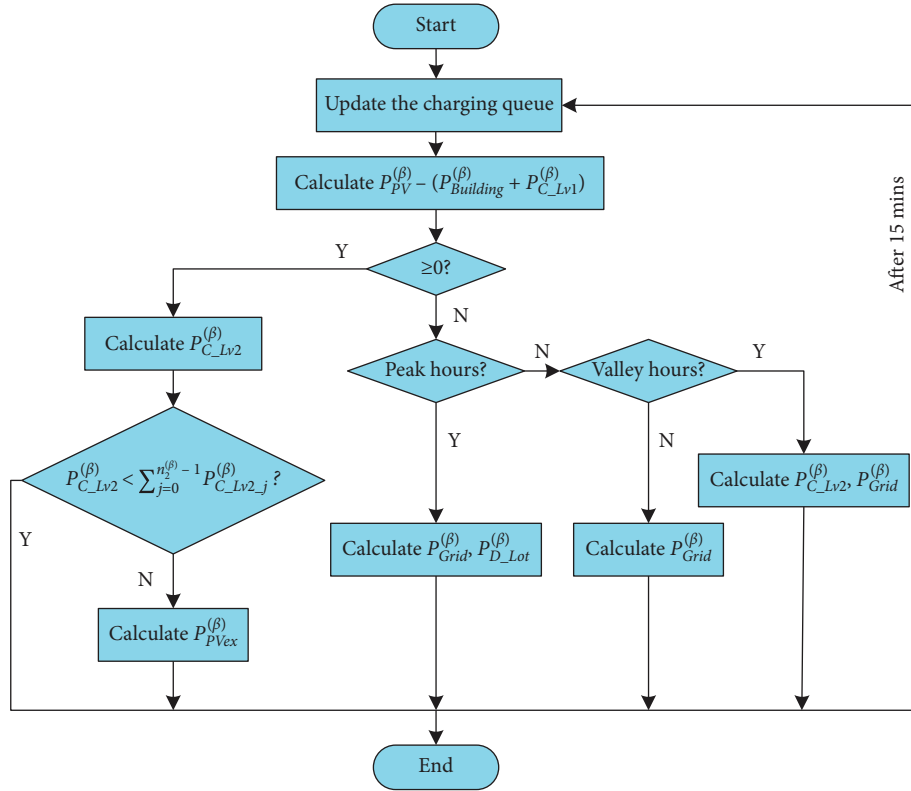


FIGURE 4: Calculation flowchart of residential areas.

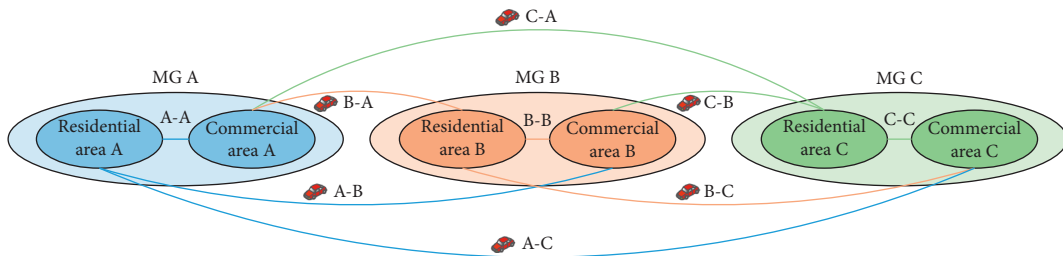


FIGURE 5: Controlled area.

MG, they are regarded as one commercial area and one residential area in a broad sense.

The simulations do not consider the physical distance between the three regional MGs but consider the commuting mileage of EVs. According to the “2018 China Urban Commuting Research Report,” 2.5 km, 10 km, 20 km, and 30 km are set as the four commuting mileages in the simulations. For the 2.5 km mileage, it is considered that the commuting destination of EVs is the nearby commercial area. The specific description is as follows:

- (1) EVs working in the nearby commercial area have a 2.5 km commuting mileage. Subordinate EVs in the MG A, B, and C all include this type. That is, the commuting mileages of A-A, B-B, and C-C are the same. 10 km, 20 km, and 30 km correspond to A-B/B-A, B-C/C-B, and C-A/A-C mileages, respectively;
- (2) The subordinate EVs in the MG A includes three commuting mileages: A-A: 2.5 km, A-B: 10 km, and A-C: 30 km;

- (3) The subordinate EVs in the MG B includes three commuting mileages: B-B: 2.5 km, B-A: 10 km, and B-C: 20 km;

- (4) The subordinate EVs in the MG C includes three commuting mileages: C-C: 2.5 km, C-B: 20 km, and C-A: 30 km;

Suppose there are 300 households in each residential area. There are 900 EVs in the entire controlled area. According to the “2018 China Urban Commuting Research Report,” approximately 31.8% of EVs (288 EVs) are allocated as A-A, B-B, and C-C mileages; 30.8% of EVs (276 EVs) are allocated as A-B/B-A mileage; 20.3% of EVs (182 EVs) are allocated as B-C/C-B mileage; 17.1% of EVs (154 EVs) are allocated as C-A/A-C mileage.

We assume that every morning, all EVs are fully charged after the last night’s valley hours, and leave the residential areas in the morning, then go to the commercial areas allocated above. In order to reflect the uncertainties of EVs’ leaving and parking, random sampling is used. At the

TABLE 1: Time distribution of EVs arriving in the commercial area.

Arrive time (t)	5:45	6:15	6:45	7:15	7:45	8:15	8:45	9:15	9:45	10:15
Probability (p) (%)	1	1.5	4	14.5	23.5	26.5	15	9	2	3

TABLE 2: Time distribution of EVs arriving in the residential area.

Arrive time (t)	16:45	17:15	17:45	18:15	18:45	19:15	19:45	20:15	20:45
Probability (p) (%)	5	13.5	18.5	26.5	14	11.5	5.5	3.5	2

beginning of each simulation, sampling a working time (the time to arrive in the commercial area in the morning) and a closing time (the time to return to the residential area at night) for each EV.

Referring to the “2017 Beijing Transportation Development Annual Report,” [29] Tables 1 and 2 are formulated, as shown in Tables 1 and 2, set the time distributions of EVs arriving in the commercial and residential areas as target distributions $\pi_1(t_1)$ and $\pi_2(t_2)$, respectively, and take proposal densities $q_1(t_1) \sim N(8.25, 1.4)$ and $q_2(t_2) \sim N(18.25, 1.4)$ for $\pi_1(t_1)$ and $\pi_2(t_2)$, respectively. Introducing the constant $M_1 = M_2 = 1$, so that $M_1 q_1(t_1)$ and $M_2 q_2(t_2)$ meet the rejection sampling principle [30]:

$$\begin{aligned} \pi_1(t_1) &\leq M_1 q_1(t_1), \\ \pi_2(t_2) &\leq M_2 q_2(t_2), \end{aligned} \quad (25)$$

where t_1 and t_2 can only take the values in Tables 1 and 2, respectively. Taking MG A as an example, the number of EVs in the commercial area A and the residential area A is obtained by random sampling, as shown in Figure 6.

Suppose every day starts at 04:45 AM and ends at 04:30 AM the next day. Updated at an interval of 15 minutes, the commuting mileages of 2.5 km, 10 km, 20 km, and 30 km are considered to be 1, 2, 3, and 4 intervals, respectively. All controlled EVs refer to Nissan LEAF 2018, which is equipped with 40 kWh battery, 3 kW charging power, and maximum mileage of 240 km [31]. According to the above travel assumptions, the SOC of each EV can be calculated.

5.2. Power Consumption Characteristics and Time-of-Use Prices. Citing the power consumption data in Ref. [27], combined with the time-of-use prices of Beijing in 2018 and [32], Table 3 is obtained. The electricity prices in valley hours, flat hours, and peak hours are marked with different colors, and the peak power consumption periods in the commercial and residential areas are highlighted.

Assuming the PV electricity price is 0, and the EV discharging price is between the valley price and the flat price, taking 0.6 RMB/kWh.

5.3. PV Simulation Data. Selecting the PV power data of a regional MG every 15 minutes on October 10, 2018 (sufficient PV power) and September 14, 2018 (fluctuating PV power) (both the commercial and residential areas are equipped with 6500 m² PV panels) as shown in Tables 4 and 5.

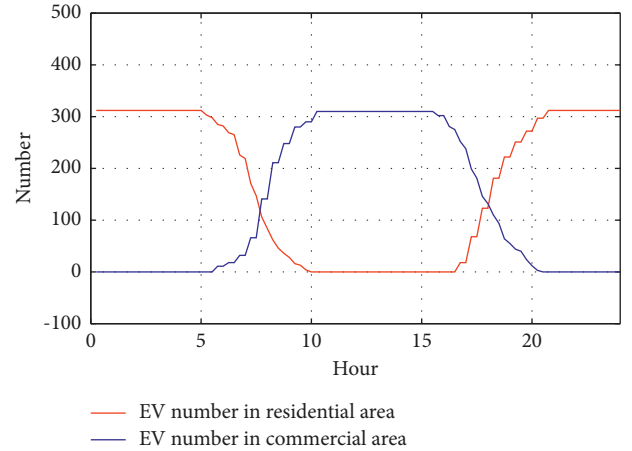


FIGURE 6: Number of EVs in commercial area A and residential area A.

TABLE 3: Power consumption characteristics.

Time	i	ii	iii
00:00	475.7	404.0	0.3748
01:00	412.3	375.2	0.3748
02:00	364.7	375.2	0.3748
03:00	348.8	404.0	0.3748
04:00	269.6	432.9	0.3748
05:00	269.6	432.9	0.3748
06:00	412.3	432.9	0.3748
07:00	539.1	432.9	0.8745
08:00	729.4	923.5	0.8745
09:00	713.5	1154.4	0.8745
10:00	713.5	1443.0	1.4002
11:00	808.7	1558.4	1.4002
12:00	824.5	1673.9	1.4002
13:00	761.1	1673.9	1.4002
14:00	745.2	1673.9	1.4002
15:00	681.8	1587.3	0.8745
16:00	666.0	1558.4	0.8745
17:00	951.4	1673.9	0.8745
18:00	1220.9	1818.2	1.4002
19:00	1331.9	1500.7	1.4002
20:00	1363.6	1298.7	1.4002
21:00	1252.6	1096.7	0.8745
22:00	1046.5	923.5	0.8745
23:00	761.1	577.2	0.3748

i: power consumption of the residential area (kW); ii: power consumption of the commercial area (kW); iii: electricity prices (RMB/kWh).

TABLE 4: PV power (10.10).

Time	P (kw)
5:15	24.7
5:30	36.3
5:45	61.1
6:00	99.2
6:15	141.3
6:30	184.5
6:45	210.2
7:00	208.7
7:15	314.7
7:30	479.4
7:45	563.8
8:00	591
8:15	535.5
8:30	607.7
8:45	645
9:00	647.7
9:15	699.4
9:30	737.3
9:45	759.6
10:00	780.3
10:15	805.4
10:30	815.6
10:45	824.3
11:00	833
11:15	841.9
11:30	842.1
11:45	843
12:00	821.7
12:15	822.9
12:30	798.8
12:45	788
13:00	768.5
13:15	756.2
13:30	664.4
13:45	607.7
14:00	535.5
14:15	591
14:30	563.8
14:45	479.4
15:00	314.7
15:15	208.7
15:30	210.2
15:45	184.5
16:00	141.3
16:15	99.2
16:30	61.1
16:45	36.3
17:00	24.7

As shown in Table 4, the PV power on October 10 is high and stable, and reach the maximum at noon.

As shown in Table 5, compared with October 10, the PV power on September 14 is lower, unstable, and fluctuates obviously.

5.4. Analysis of Simulation Results. Each commercial area (residential area) is similar, so only select the simulation results of the MG A for analysis. It should be noted that since the commuting time of 900 EVs will be randomly sampled at

TABLE 5: PV power (09.14).

Time	P (kw)
6:30	8.4
6:45	11.9
7:00	25
7:15	74.2
7:30	132.7
7:45	173.9
8:00	110.6
8:15	82.2
8:30	119
8:45	150
9:00	247.5
9:15	450.2
9:30	455.2
9:45	511.6
10:00	560.6
10:15	558.9
10:30	364.3
10:45	469.4
11:00	242.7
11:15	392.1
11:30	563
11:45	183.8
12:00	113.1
12:15	137.4
12:30	199.1
12:45	138.1
13:00	146.3
13:15	272.2
13:30	370.9
13:45	445.7
14:00	334
14:15	368
14:30	496.3
14:45	450.2
15:00	247.5
15:15	150
15:30	119
15:45	82.2
16:00	110.6
16:15	173.9
16:30	132.7
16:45	74.2
17:00	25
17:15	11.9
17:30	8.4

the beginning of each simulation, although similar results can be obtained, there will be a little difference in specific values.

5.4.1. Case 1: Regulation Effect with Sufficient PV Power. The PV power on October 10 is stable and sufficient. The regulation effect of the proposed strategy is shown in Figure 7. In Figure 7(a) and the following figures, the “Without PV and EV” curve represents the power consumption (in the simulation analysis of this paper, power consumption is regarded as the power imported from the power grid) when neither PV generations nor EVs is added, the “With PV only” curve represents the

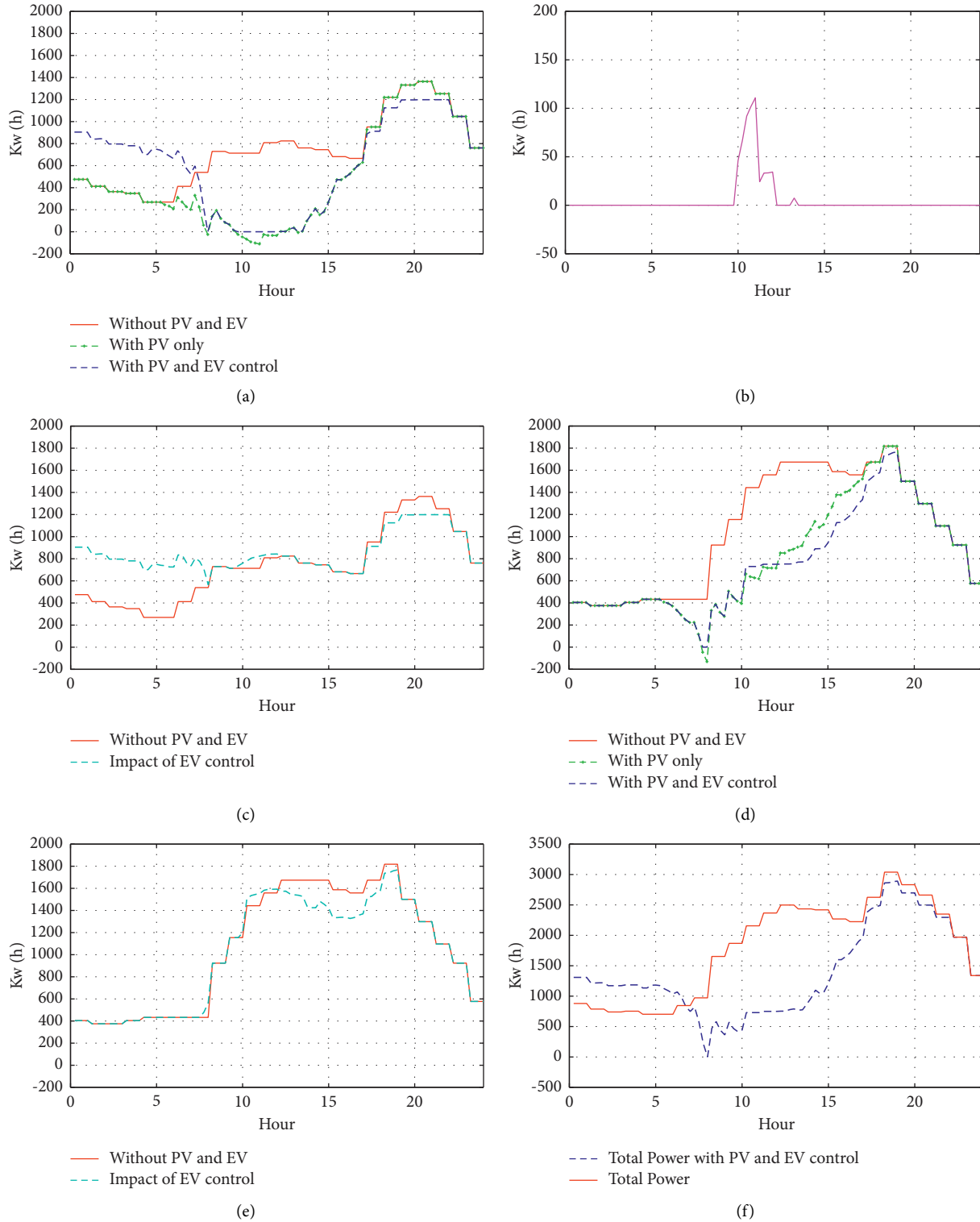


FIGURE 7: Regulation effect with sufficient PV power (10.10). (a) Regulation effect in the residential area. (b) Excess PV power in the residential area. (c) EV charging-discharging effect in the residential area. (d) Regulation effect in the commercial area. (e) EV charging-discharging effect in the commercial area. (f) Total power consumption before and after regulation.

power consumption when only PV generations added without EVs, the “With PV and EV control” curve represents the power consumption after PV generations and EVs are added, and the “Impact of EV control” curve

represents the regulation effect of EVs charging and discharging.

Figure 7(a) shows that the addition of PV generations greatly reduces the power consumption of the residential

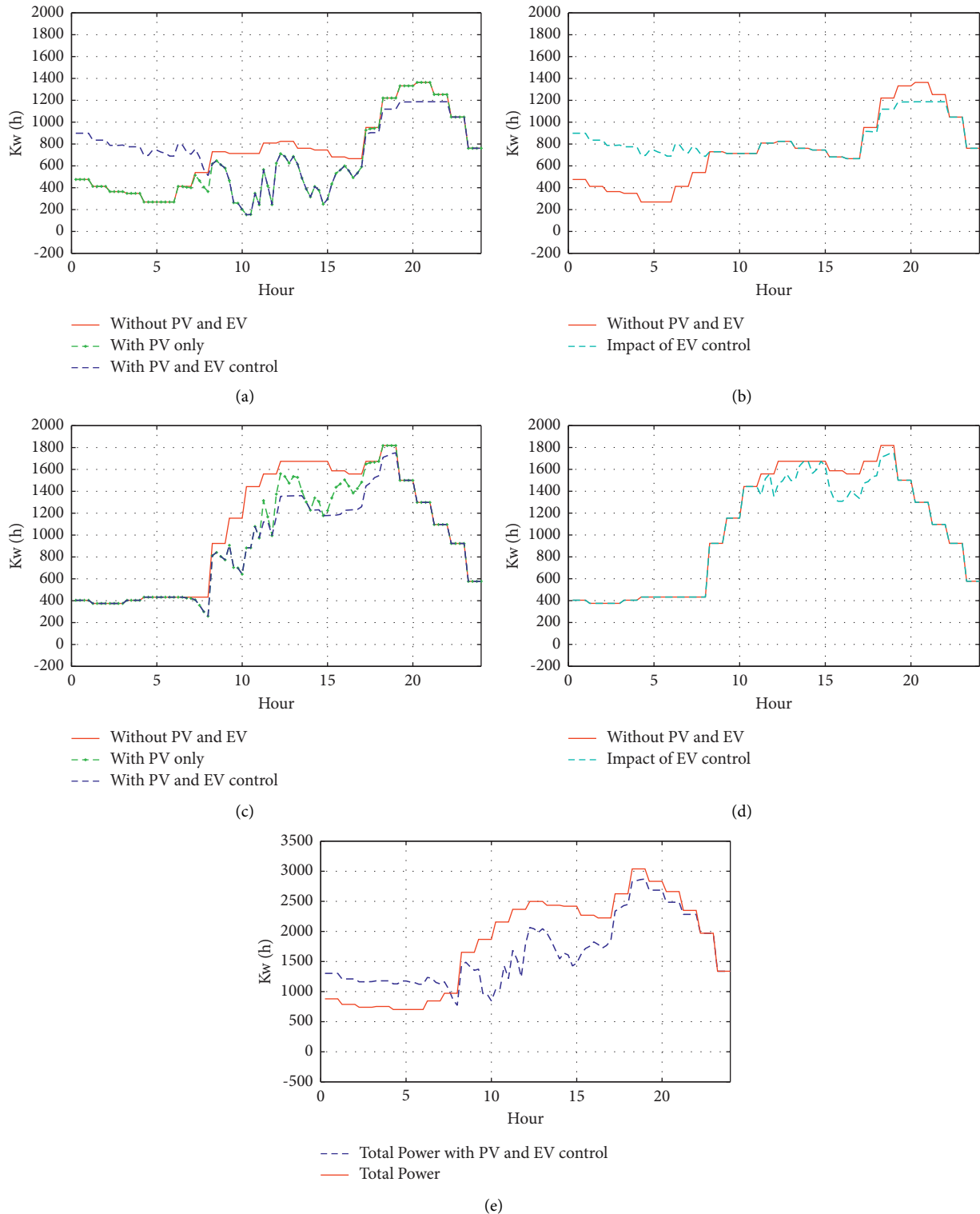


FIGURE 8: Regulation effect with fluctuating PV power (09.14). (a) Regulation effect in the residential area. (b) EV charging-discharging effect in the residential area. (c) Regulation effect in the commercial area. (d) EV charging-discharging effect in the commercial area. (e) Total power consumption before and after regulation.

area during the daytime (06:00–16:00). However, due to the PV panels can not work at night. So it has no effect. By adding EVs, the peak power consumption at night (18:00–22:00) is reduced. On the other hand, the orderly

charging of EVs during 00:00–08:00 in the residential area effectively realizes valley filling.

Figure 7(b) shows that the local PV power has exceeded the load demand, which is the part less than 0 in the “With

PV only” curve in Figure 7(a). This part of the power will be transmitted to the nearby commercial area. In about 2 hours at noon, due to the high output of PV panels, the residential area provides some PV power to the commercial area, and the highest instantaneous power exceeds 100 kW.

Figure 7(c) shows the EV charging-discharging effect on the power consumption of the residential area. During 00:00–08:00, after valley filling, the power consumption is close to that during daytime flat hours. During 18:00–22:00, the discharging of EVs also realizes peak shaving. During 08:00–18:00, EVs are concentrated in the commercial area, so there is almost no regulation effect.

Figure 7(d) shows the regulation effect of the proposed strategy in the commercial area. The PV power effectively reduces the power consumption during the daytime (05:00–17:00). The part less than 0 in the “With PV only” curve before the 8th hour represents that the local PV power has exceeded the load demand at this time. This part of the power will be used to charge EVs in the commercial area, which is reflected in the “With PV and EV control” curve. The “With PV and EV control” curve shows the orderly discharging of EVs further reduces the power consumption during daytime peak hours (10:00–18:00). At night, PV panels stop working, at the same time, EVs leave the commercial area and return to the residential area, so the regulation effect decreases.

Figure 7(e) shows the EV charging-discharging effect on the power consumption of the commercial area. During 10:00–18:00, the orderly discharging of EVs realizes a certain degree of peak shaving. This part of discharging power mainly comes from the electric energy stored by EVs in the residential area from 00:00–08:00. During 00:00–10:00 and 18:00–24:00, EVs are concentrated in the residential area, so there is almost no regulation effect.

Figure 7(f) shows the comparison of the total power consumption of the MG A before and after regulation, which are represented by the “Total Power” curve and the “Total Power with PV and EV control” curve, respectively. From 00:00 to 07:00, the orderly charging of EVs in the residential area realizes valley filling. Due to the PV power and EV discharging, the power consumption during the daytime decreases significantly. During night peak hours (18:00–22:00), EV discharging also has a certain effect on peak shaving.

In terms of economy, after the regulation, the whole day electricity bills in the residential area were reduced by 33% and that in the commercial area by 27%. The strategy proposed in this paper can effectively improve the economy of the regional MG.

5.4.2. Case 2: Regulation Effect with Fluctuating PV Power. The PV power on September 14 is low and fluctuates, obviously. The regulation effect of the proposed strategy in the residential area is shown in Figure 8.

Figure 8(a) shows that although PV power significantly reduces the power consumption of the residential area, it has obvious fluctuations compared with Figure 7(a). Due to the low output of PV panels, there is no excess PV power all day.

Figure 8(b) shows the EV charging-discharging effect on the power consumption of the residential area. Figure 8(b) is similar to Figure 7(c), which shows that during 00:00–08:00 and 18:00–22:00, because PV generations can not work, so the peak shaving and valley filling effects of EVs are less affected.

Figure 8(c) shows the regulation effect of the proposed strategy in the commercial area. The “With PV only” curve shows that although PV power reduces power consumption during the daytime, it causes obvious fluctuations due to its own instability. From the 11th hour, EVs begin to discharge, so the power consumption of the commercial area is further reduced. On the other hand, the “With PV and EV control” curve is more stable than the “With PV only” curve because equation (17) has the function of reducing fluctuations. This result also points out that EV charging-discharging can effectively reduce power fluctuations and improve stability.

Figure 8(d) shows the EV charging-discharging effect on the power consumption of the commercial area. The difference between Figures 8(d) and 7(e) is that on September 14, the discharging power of EVs fluctuated significantly, which shows that the discharging power can make adjustments to the fluctuations caused by the instability of PV power.

Figure 8(e) shows the comparison of the total power consumption of the MG A before and after regulation. The effects of valley filling during 00:00–06:00 and peak shaving during 18:00–22:00 are similar to Figure 7(f). However, due to the instability of PV power on September 14, total power consumption during the daytime has obvious fluctuations. Since in the commercial area, the discharging of EVs during the daytime has suppressed the fluctuations to a certain extent, the fluctuations in total power consumption mainly comes from residential areas. In terms of the economy, after the regulation, the whole day electricity bills in the residential area were reduced by 13% and in the commercial area by 16%. The regulation strategy proposed in this paper can improve the economy of the regional MG when PV power fluctuates.

6. Conclusions

EVs have exhibited promising potential in power regulation. We propose a regional MG optimal scheduling strategy considering EVs as mobile energy storage. Further, power consumption models of commercial and residential areas and the charge-discharge model of EVs are, respectively, established. The simulations are performed under two cases: stable PV power and fluctuating PV power, and we use random sampling to imitate the behavior characteristics of EVs. The results from two case studies have been analyzed, which show that the charging-discharging of EVs can be flexibly adjusted to realize peak shaving and valley filling. Meanwhile, PV energy deployment between different subareas can better consume renewable energy. Case 2 shows that the discharging of EVs can also stabilize power fluctuations. In two cases, the proposed strategy can improve the economic benefits of the regional MG.

This paper assumes that all EVs are allowed to participate in optimal scheduling without considering the influence of EV owners on EVs charging and discharging. Future research will focus on how to analyze the impact of human factors on the charging-discharging of EVs.

Nomenclature

MG: Microgrid
 EV: Electric vehicle
 RES: Renewable energy source
 V2G: Vehicle-to-grid
 BV: Battery vehicle
 PV: Photovoltaic
 SOC: State of charge.

Indices

α : Commercial area
 β : Residential area
 t : Time.

Parameters

$P_C^{(\alpha)}$ ($P_C^{(\beta)}$): Power consumed by commercial area
 $P_O^{(\alpha)}$ ($P_O^{(\beta)}$): Power obtained by residential area
 $P_{\text{Building}}^{(\alpha)}$ ($P_{\text{Building}}^{(\beta)}$): Power consumed by commercial (residential) buildings
 $P_{C_Lot}^{(\alpha)}$ ($P_{C_Lot}^{(\beta)}$): Charging power of commercial (residential) parking lot
 $P_{PV}^{(\alpha)}$ ($P_{PV}^{(\beta)}$): PV power in commercial (residential) area
 $P_{D_Lot}^{(\alpha)}$ ($P_{D_Lot}^{(\beta)}$): Discharging power of commercial (residential) parking lots
 $P_{\text{Grid}}^{(\alpha)}$ ($P_{\text{Grid}}^{(\beta)}$): Power imported from power grid by commercial (residential) area
 $P_{PVex}^{(\beta)}$: Excess PV power in residential area
 L : Capacity of each vehicle
 $P_{C_Lv1}^{(\alpha)}$ ($P_{C_Lv1}^{(\beta)}$): Total charging power of EVs in Lv1 in commercial (residential) area
 $P_{C_Lv2}^{(\alpha)}$ ($P_{C_Lv2}^{(\beta)}$): Total charging power of EVs in Lv2 in commercial (residential) area
 $n_1^{(\alpha)}$ ($n_1^{(\beta)}$): Number of EVs in Lv1 in commercial (residential) area
 $n_2^{(\alpha)}$ ($n_2^{(\beta)}$): Number of EVs in Lv2 in commercial (residential) area
 $n_3^{(\alpha)}$ ($n_3^{(\beta)}$): Number of EVs in Lv3 in commercial (residential) area
 $P_{C_Lv1-i}^{(\alpha)}$ ($P_{C_Lv1-i}^{(\beta)}$): Charging power of the i th EV in Lv1 in commercial (residential) area
 $P_{C_Lv2-j}^{(\alpha)}$ ($P_{C_Lv2-j}^{(\beta)}$): Charging power of the j th EV in Lv2 in commercial (residential) area
 $SOC_{Lv3-k}^{(\alpha)}$ ($SOC_{Lv3-k}^{(\beta)}$): SOC of the k th EV in Lv3 in commercial (residential) area
 $P_{D_Lv3-k}^{(\alpha)}$ ($P_{D_Lv3-k}^{(\beta)}$): Discharging power of the k th EV in Lv3 in commercial (residential) area
 $t_{pd-\alpha}$ ($t_{pd-\beta}$): End of the peak hours in commercial (residential) area

$t_{vd-\beta}$: End of the valley hours in residential area.

Data Availability

The data that support the findings of this study are available from the corresponding author upon reasonable request.

Conflicts of Interest

The authors declare that there are no conflicts of interest regarding the publication of this paper.

Acknowledgments

This work was supported by the National Natural Science Foundation of China (62073173, 61973151, and 61833011) and the Natural Science Foundation of Jiangsu Province, China (BK20191376 and BK20191406).

References

- [1] K. Kumar, L. Varshney, A. Ambikapathy, R. K. Saket, and S. Mekhilef, "Solar tracker transcript—a review," *International Transactions on Electrical Energy Systems*, vol. 31, no. 12, Article ID e13250, 2021.
- [2] V. Nikam and V. Kalkhambkar, "A review on control strategies for microgrids with distributed energy resources, energy storage systems, and electric vehicles," *International Transactions on Electrical Energy Systems*, vol. 31, Article ID e12607, 2021.
- [3] Y. Xue, "Energy internet or comprehensive energy network?" *Journal of Modern Power Systems and Clean Energy*, vol. 3, no. 3, pp. 297–301, 2015.
- [4] S. Choudhury, "A comprehensive review on issues, investigations, control and protection trends, technical challenges and future directions for Microgrid technology," *International Transactions on Electrical Energy Systems*, vol. 30, Article ID e12446, 2020.
- [5] X. Zhou, Q. Ai, and H. Wang, "A distributed dispatch method for microgrid cluster considering demand response," *International Transactions on Electrical Energy Systems*, vol. 28, Article ID e2634, 2018.
- [6] J. Ma, X. Liu, and Y. Chen, "Current status and countermeasures for China's new energy automobile industry and technology Development," *China Journal of Highway and Transport*, vol. 31, no. 8, pp. 1–19, 2018.
- [7] S. Kong, Z. Hu, S. Xie, L. Yang, and Y. Zheng, "Two-stage robust planning model and its solution algorithm of active distribution network containing electric vehicle charging stations," *Transactions of China Electrotechnical Society*, vol. 35, no. 5, pp. 179–191, 2020.
- [8] W. Shi, L. Lv, and H. Gao, "Economic dispatch of active distribution network with participation of demand response and electric vehicle," *Automation of Electric Power Systems*, vol. 44, no. 11, pp. 41–51, 2020.
- [9] L. Ren, Z. Song, C. Mao, and F. Liu, "Multitime scale coordinated scheduling for electric vehicles considering photovoltaic/wind/battery generation in microgrid," *International Transactions on Electrical Energy Systems*, vol. 29, Article ID e2821, 2019.
- [10] L. Shi, T. Lv, and Y. Wang, "Vehicle-to-grid service development logic and management formulation," *Journal of*

- Modern Power System and Clean Energy*, vol. 7, no. 4, pp. 935–947, 2019.
- [11] W. Liu, S. Chen, Y. Hou, and Z. Yang, “Optimal reserve management of electric vehicle aggregator: discrete bilevel optimization model and exact algorithm,” *IEEE Transactions on Smart Grid*, vol. 12, no. 5, pp. 4003–4015, 2021.
- [12] Y. Ota, H. Taniguchi, J. Baba, and A. Yokoyama, “Implementation of autonomous distributed V2G to electric vehicle and DC charging system,” *Electric Power Systems Research*, vol. 120, pp. 177–183, 2015.
- [13] S. Han, S. Han, and K. Sezaki, “Estimation of achievable power capacity from plug-in electric vehicles for V2G frequency regulation: case studies for market participation,” *IEEE Transactions on Smart Grid*, vol. 2, no. 4, pp. 632–641, 2011.
- [14] S. Iqbal, A. Xin, and M. U. Jan, “Aggregation of EVs for primary frequency control of an industrial microgrid by implementing grid regulation & charger controller,” *IEEE Access*, vol. 8, pp. 141977–141989, 2020.
- [15] X. Deng, Q. Zhang, Y. Li, T. Sun, and H. Yue, “Hierarchical distributed frequency regulation strategy of electric vehicle cluster considering demand charging load optimization,” *IEEE Transactions on Industry Applications*, vol. 58, no. 1, pp. 720–731, 2022.
- [16] S. Sachan and M. H. Amini, “Optimal allocation of EV charging spots along with capacitors in smart distribution network for congestion management,” *International Transactions on Electrical Energy Systems*, vol. 30, Article ID e12507, 2020.
- [17] M. A. López, S. de la Torre, S. Martín, and J. A. Aguado, “Demand-side management in smart grid operation considering electric vehicles load shifting and vehicle-to-grid support,” *International Journal of Electrical Power & Energy Systems*, vol. 64, pp. 689–698, 2015.
- [18] J. Kester, N. Lance, X. Lin, G. Z. Rubens, and B. K. Sovacool, “The coproduction of electric mobility: selectivity, conformity and fragmentation in the sociotechnical acceptance of vehicle-to-grid (V2G) standards,” *Journal of Cleaner Production*, vol. 207, pp. 400–410, 2019.
- [19] H. Hou, M. Xue, and Y. Xu, “Multi-objective economic dispatch of a microgrid considering electric vehicle and transferable load,” *Applied Energy*, vol. 262, Article ID 114489, 2020.
- [20] N. I. Nimalsiri, E. L. Ratnam, D. B. Smith, C. P. Mediwaththe, and S. K. Halgamuge, “Coordinated charge and discharge scheduling of electric vehicles for load curve shaping,” *IEEE Transactions on Intelligent Transportation Systems*, vol. 23, no. 7, pp. 7653–7665, 2021.
- [21] K. N. Qureshi, A. Alhudhaif, and G. Jeon, “Electric-vehicle energy management and charging scheduling system in sustainable cities and society,” *Sustainable Cities and Society*, vol. 71, Article ID 102990, 2021.
- [22] Y. Li, M. Han, Z. Yang, and G. Li, “Coordinating flexible demand response and renewable uncertainties for scheduling of community integrated energy systems with an electric vehicle charging station: a bi-level approach,” *IEEE Transactions on Sustainable Energy*, vol. 12, no. 4, pp. 2321–2331, 2021.
- [23] Z. Liu, Q. Wu, and M. Shahidehpour, “Transactive real-time electric vehicle charging management for commercial buildings with PV on-site generation,” *IEEE Transactions on Smart Grid*, vol. 10, no. 5, pp. 4939–4950, 2018.
- [24] U. C. Chukwu and S. M. Mahajan, “V2G parking lot with PV rooftop for capacity enhancement of a distribution system,” *IEEE Transactions on Sustainable Energy*, vol. 5, no. 1, pp. 119–127, 2014.
- [25] L. Drude, L. C. Pereira Junior, and R. Rütther, “Photovoltaics (PV) and electric vehicle-to-grid (V2G) strategies for peak demand reduction in urban regions in Brazil in a smart grid environment,” *Renewable Energy*, vol. 68, pp. 443–451, 2014.
- [26] W. Zhong, R. Yu, S. Xie, Y. Zhang, and D. K. Y. Yau, “On stability and robustness of demand response in V2G mobile energy networks,” *IEEE Transactions on Smart Grid*, vol. 9, no. 4, pp. 3203–3212, 2018.
- [27] T. Logenthiran, D. Srinivasan, and T. Z. Shun, “Demand side management in smart grid using heuristic optimization,” *IEEE Transactions on Smart Grid*, vol. 3, no. 3, pp. 1244–1252, 2012.
- [28] S. Singh, P. Chauhan, and N. J. Singh, “Feasibility of grid-connected solar-wind hybrid system with electric vehicle charging station,” *Journal of Modern Power Systems and Clean Energy*, vol. 9, no. 2, pp. 295–306, 2021.
- [29] Beijing Transportation Development Annual Report, <http://www.bjtrc.org.cn/>.
- [30] S. Huang, C. Ye, and S. Liu, “Data-driven reliability assessment of an electric vehicle penetrated grid utilizing the diffusion estimator and slice sampling,” *CSEE Journal of Power and Energy Systems (Early Access)*, 2020.
- [31] J. Su, T. T. Lie, and R. Zamora, “Modelling of large-scale electric vehicles charging demand: a New Zealand case study,” *Electric Power Systems Research*, vol. 167, pp. 171–182, 2019.
- [32] D. Wei, C. Zhang, B. Su, and N. Cui, “A time-of-use price based multi-objective optimal dispatching for charging and discharging of electric vehicles,” *Power System Technology*, vol. 38, no. 11, pp. 2972–2977, 2014.